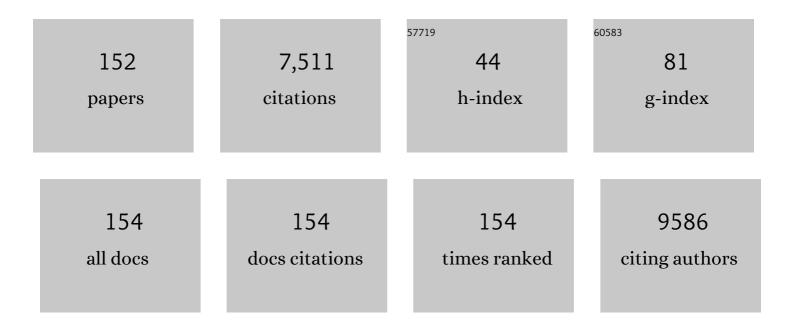
Zhongyuan Liu

List of Publications by Year in descending order

Source: https://exaly.com/author-pdf/5077065/publications.pdf Version: 2024-02-01



| # | Article | IF | CITATIONS |
|----|--|------|-----------|
| 1 | Ultrahard nanotwinned cubic boron nitride. Nature, 2013, 493, 385-388. | 13.7 | 662 |
| 2 | Nanotwinned diamond with unprecedented hardness and stability. Nature, 2014, 510, 250-253. | 13.7 | 611 |
| 3 | Investigation on Microwave Absorption Properties for Multiwalled Carbon Nanotubes/Fe/Co/Ni Nanopowders as Lightweight Absorbers. Journal of Physical Chemistry C, 2011, 115, 14025-14030. | 1.5 | 448 |
| 4 | Flexible Allâ€Solidâ€State Supercapacitors based on Liquidâ€Exfoliated Blackâ€Phosphorus Nanoflakes. Advanced Materials, 2016, 28, 3194-3201. | 11.1 | 290 |
| 5 | Teâ€Doped Black Phosphorus Fieldâ€Effect Transistors. Advanced Materials, 2016, 28, 9408-9415. | 11.1 | 241 |
| 6 | Microwave Absorption Properties of CoS ₂ Nanocrystals Embedded into Reduced Graphene Oxide. ACS Applied Materials & Interfaces, 2017, 9, 28868-28875. | 4.0 | 215 |
| 7 | Hardness of covalent compounds: Roles of metallic component and d valence electrons. Journal of Applied Physics, 2008, 104, . | 1.1 | 166 |
| 8 | Liquidâ€Exfoliated Black Phosphorous Nanosheet Thin Films for Flexible Resistive Random Access Memory Applications. Advanced Functional Materials, 2016, 26, 2016-2024. | 7.8 | 161 |
| 9 | Controlled Incorporation of Ni(OH) ₂ Nanoplates Into Flowerlike MoS ₂ Nanosheets for Flexible Allâ€Solidâ€State Supercapacitors. Advanced Functional Materials, 2014, 24, 6700-6707. | 7.8 | 145 |
| 10 | Enhanced laser scribed flexible graphene-based micro-supercapacitor performance with reduction of carbon nanotubes diameter. Carbon, 2014, 75, 236-243. | 5.4 | 139 |
| 11 | Nonvolatile Ferroelectric Memory Effect in Ultrathin αâ€In ₂ Se ₃ . Advanced Functional Materials, 2019, 29, 1808606. | 7.8 | 137 |
| 12 | Broadband Black Phosphorus Optical Modulator in the Spectral Range from Visible to Midâ€infrared. Advanced Optical Materials, 2015, 3, 1787-1792. | 3.6 | 115 |
| 13 | Fabrication of carbon encapsulated Co 3 O 4 nanoparticles embedded in porous graphitic carbon nanosheets for microwave absorber. Carbon, 2015, 89, 372-377. | 5.4 | 114 |
| 14 | Fabrication of NiCo ₂ -Anchored Graphene Nanosheets by Liquid-Phase Exfoliation for Excellent Microwave Absorbers. ACS Applied Materials & Interfaces, 2017, 9, 12673-12679. | 4.0 | 111 |
| 15 | Compressed glassy carbon: An ultrastrong and elastic interpenetrating graphene network. Science Advances, 2017, 3, e1603213. | 4.7 | 110 |
| 16 | Enhanced stability of black phosphorus field-effect transistors with SiO ₂ passivation. Nanotechnology, 2015, 26, 435702. | 1.3 | 102 |
| 17 | Blackâ€Phosphorusâ€Incorporated Hydrogel as a Conductive and Biodegradable Platform for Enhancement of the Neural Differentiation of Mesenchymal Stem Cells. Advanced Functional Materials, 2020, 30, 2000177. | 7.8 | 100 |
| 18 | Microwave Synthesized Three-dimensional Hierarchical Nanostructure CoS2/MoS2 Growth on Carbon Fiber Cloth: A Bifunctional Electrode for Hydrogen Evolution Reaction and Supercapacitor. Electrochimica Acta, 2016, 212, 941-949. | 2.6 | 93 |

| # | Article | IF | CITATIONS |
|----|--|-----|-----------|
| 19 | Sulfur-Doped Black Phosphorus Field-Effect Transistors with Enhanced Stability. ACS Applied Materials & Interfaces, 2018, 10, 9663-9668. | 4.0 | 93 |
| 20 | Enhanced Photoresponse of SnSe-Nanocrystals-Decorated WS ₂ Monolayer Phototransistor. ACS Applied Materials & Interfaces, 2016, 8, 4781-4788. | 4.0 | 91 |
| 21 | Flexible Black-Phosphorus Nanoflake/Carbon Nanotube Composite Paper for High-Performance All-Solid-State Supercapacitors. ACS Applied Materials & Interfaces, 2017, 9, 44478-44484. | 4.0 | 89 |
| 22 | First-principles studies of structural and electronic properties of hexagonalBC5. Physical Review B, 2006, 73, . | 1.1 | 75 |
| 23 | Microwave absorption properties of multiwalled carbon nanotube/FeNi nanopowders as light-weight microwave absorbers. Journal of Magnetism and Magnetic Materials, 2013, 343, 281-285. | 1.0 | 74 |
| 24 | Approaching diamond's theoretical elasticity and strength limits. Nature Communications, 2019, 10, 5533. | 5.8 | 73 |
| 25 | Enhanced thermoelectric figure of merit in nanocrystalline Bi2Te3 bulk. Journal of Applied Physics, 2009, 105, . | 1.1 | 71 |
| 26 | Two-dimensional materials and one-dimensional carbon nanotube composites for microwave absorption. Nanotechnology, 2018, 29, 025704. | 1.3 | 71 |
| 27 | Atomically Resolving Polymorphs and Crystal Structures of In ₂ Se ₃ . Chemistry of Materials, 2019, 31, 10143-10149. | 3.2 | 71 |
| 28 | Carbon-Encapsulated Co 3 O 4 @CoO@Co Nanocomposites for Multifunctional Applications in Enhanced Long-life Lithium Storage, Supercapacitor and Oxygen Evolution Reaction. Electrochimica Acta, 2016, 220, 322-330. | 2.6 | 68 |
| 29 | Lateral Bilayer MoS ₂ –WS ₂ Heterostructure Photodetectors with High Responsivity and Detectivity. Advanced Optical Materials, 2019, 7, 1900815. | 3.6 | 65 |
| 30 | Twoâ€Dimensionalâ€Germanium Phosphideâ€Reinforced Conductive and Biodegradable Hydrogel Scaffolds Enhance Spinal Cord Injury Repair. Advanced Functional Materials, 2021, 31, 2104440. | 7.8 | 65 |
| 31 | Microwave synthesized self-standing electrode of MoS 2 nanosheets assembled on graphene foam for high-performance Li-lon and Na-Ion batteries. Journal of Alloys and Compounds, 2016, 660, 11-16. | 2.8 | 64 |
| 32 | Gate tunable MoS ₂ –black phosphorus heterojunction devices. 2D Materials, 2015, 2, 034009. | 2.0 | 61 |
| 33 | Gate tunable WSe ₂ –BP van der Waals heterojunction devices. Nanoscale, 2016, 8, 3254-3258. | 2.8 | 60 |
| 34 | Mechanical properties of nanocrystalline TiC–ZrC solid solutions fabricated by spark plasma sintering. Ceramics International, 2014, 40, 10517-10522. | 2.3 | 57 |
| 35 | SnS 2 Nanoflakes Anchored Graphene obtained by Liquid Phase Exfoliation and MoS 2 Nanosheet Composites as Lithium and Sodium Battery Anodes. Electrochimica Acta, 2017, 227, 203-209. | 2.6 | 57 |
| 36 | Atomic-Scale Observation of Reversible Thermally Driven Phase Transformation in 2D In ₂ Se ₃ . ACS Nano, 2019, 13, 8004-8011. | 7.3 | 57 |

| # | Article | IF | CITATIONS |
|----|--|-----|-----------|
| 37 | Orthogonal Electric Control of the Outâ€Ofâ€Plane Fieldâ€Effect in 2D Ferroelectric αâ€In ₂ Se ₃ . Advanced Electronic Materials, 2020, 6, 2000061. | 2.6 | 56 |
| 38 | Sodium-Induced Reordering of Atomic Stacks in Black Phosphorus. Chemistry of Materials, 2017, 29, 1350-1356. | 3.2 | 55 |
| 39 | Degradation of black phosphorus: a real-time ³¹ P NMR study. 2D Materials, 2016, 3, 035025. | 2.0 | 53 |
| 40 | Prediction of a sandwichlike conducting superhard boron carbide: First-principles calculations. Physical Review B, 2006, 73, . | 1.1 | 48 |
| 41 | Direct Observation of Room-Temperature Dislocation Plasticity in Diamond. Matter, 2020, 2, 1222-1232. | 5.0 | 48 |
| 42 | Great thermoelectric power factor enhancement of CoSb3 through the lightest metal element filling. Applied Physics Letters, 2011, 98, . | 1.5 | 47 |
| 43 | Application of hard ceramic materials B4C in energy storage: Design B4C@C core-shell nanoparticles as electrodes for flexible all-solid-state micro-supercapacitors with ultrahigh cyclability. Nano Energy, 2020, 75, 104947. | 8.2 | 47 |
| 44 | Compressive Strength of Diamond from First-Principles Calculation. Journal of Physical Chemistry C, 2010, 114, 17851-17853. | 1.5 | 46 |
| 45 | Bulk Re ₂ C: Crystal Structure, Hardness, and Ultra-incompressibility. Crystal Growth and Design, 2010, 10, 5024-5026. | 1.4 | 46 |
| 46 | Photodetectors based on sensitized two-dimensional transition metal dichalcogenides—A review. Journal of Materials Research, 2017, 32, 4115-4131. | 1.2 | 46 |
| 47 | Facile synthesis and excellent electrochemical performance of CoP nanowire on carbon cloth as bifunctional electrode for hydrogen evolution reaction and supercapacitor. Science China Materials, 2017, 60, 1179-1186. | 3.5 | 42 |
| 48 | Grain-boundary-rich polycrystalline monolayer WS2 film for attomolar-level Hg2+ sensors. Nature Communications, 2021, 12, 3870. | 5.8 | 42 |
| 49 | Chalcopyrite polymorph for superhard BC2N. Applied Physics Letters, 2006, 89, 151911. | 1.5 | 41 |
| 50 | Superior microwave absorption properties of ultralight reduced graphene oxide/black phosphorus aerogel. Nanotechnology, 2018, 29, 235604. | 1.3 | 41 |
| 51 | Highly sensitive and fast monolayer WS ₂ phototransistors realized by SnS nanosheet decoration. Nanoscale, 2017, 9, 1916-1924. | 2.8 | 39 |
| 52 | Structure and mechanical properties of osmium carbide: First-principles calculations. Applied Physics Letters, 2008, 93, . | 1.5 | 38 |
| 53 | 2D Hybrid Superlattice-Based On-Chip Electrocatalytic Microdevice for <i>in Situ</i> Revealing Enhanced Catalytic Activity. ACS Nano, 2020, 14, 1635-1644. | 7.3 | 36 |
| 54 | Two-dimensional black phosphorous induced exciton dissociation efficiency enhancement for high-performance all-inorganic CsPbl ₃ perovskite photovoltaics. Journal of Materials Chemistry A, 2019, 7, 22539-22549. | 5.2 | 35 |

| # | Article | IF | CITATIONS |
|----|---|-----|-----------|
| 55 | Well-controlled Core-shell structures based on Fe3O4 nanospheres coated by polyaniline for highly efficient microwave absorption. Applied Surface Science, 2022, 591, 153176. | 3.1 | 35 |
| 56 | Chemical Vapor Synthesized WS2-Embedded Polystyrene-derived Porous Carbon as Superior Long-term Cycling Life Anode Material for Li-ion Batteries. Electrochimica Acta, 2015, 153, 49-54. | 2.6 | 33 |
| 57 | Narrowing Working Voltage Window to Improve Layered GeP Anode Cycling Performance for Lithium-Ion Batteries. ACS Applied Materials & Interfaces, 2020, 12, 17466-17473. | 4.0 | 33 |
| 58 | A tetragonal phase of superhard BC2N. Journal of Applied Physics, 2009, 105, . | 1.1 | 32 |
| 59 | Liquid-exfoliation of S-doped black phosphorus nanosheets for enhanced oxygen evolution catalysis. Nanotechnology, 2019, 30, 035701. | 1.3 | 32 |
| 60 | Porous bismuth antimony telluride alloys with excellent thermoelectric and mechanical properties. Journal of Materials Chemistry A, 2021, 9, 4990-4999. | 5.2 | 32 |
| 61 | Microwave synthesis of SnS2 nanoflakes anchored graphene foam for flexible lithium-ion battery anodes with long cycling life. Materials Letters, 2016, 174, 24-27. | 1.3 | 31 |
| 62 | Microwave absorption characteristics of CH3NH3PbI3 perovskite/carbon nanotube composites. Journal of Materials Science, 2017, 52, 13023-13032. | 1.7 | 31 |
| 63 | Metallic layered germanium phosphide GeP ₅ for high rate flexible all-solid-state supercapacitors. Journal of Materials Chemistry A, 2018, 6, 19409-19416. | 5.2 | 31 |
| 64 | Metal–organic framework derived cobalt phosphosulfide with ultrahigh microwave absorption properties. Nanotechnology, 2018, 29, 405703. | 1.3 | 30 |
| 65 | Direct large-scale fabrication of C-encapsulated B4C nanoparticles with tunable dielectric properties as excellent microwave absorbers. Carbon, 2019, 148, 504-511. | 5.4 | 30 |
| 66 | Fabrication of multifunctional carbon encapsulated Ni@NiO nanocomposites for oxygen reduction, oxygen evolution and lithium-ion battery anode materials. Science China Materials, 2017, 60, 947-954. | 3.5 | 29 |
| 67 | Enhanced thermoelectric performance of Na-doped PbTe synthesized under high pressure. Science China Materials, 2018, 61, 1218-1224. | 3.5 | 29 |
| 68 | Spark plasma sintering of the nonstoichiometric ultrafine-grained titanium carbides with nano superstructural domains of the ordered carbon vacancies. Materials Chemistry and Physics, 2011, 130, 352-360. | 2.0 | 28 |
| 69 | Superstructural nanodomains of ordered carbon vacancies in nonstoichiometric ZrC _{0.61} . Journal of Materials Research, 2012, 27, 1230-1236. | 1.2 | 28 |
| 70 | Large and Anisotropic Linear Magnetoresistance in Single Crystals of Black Phosphorus Arising From Mobility Fluctuations. Scientific Reports, 2016, 6, 23807. | 1.6 | 26 |
| 71 | Ultrahigh-Gain and Fast Photodetectors Built on Atomically Thin Bilayer Tungsten Disulfide Grown by Chemical Vapor Deposition. ACS Applied Materials & Interfaces, 2017, 9, 42001-42010. | 4.0 | 26 |
| 72 | Ambipolar Photoresponsivity in an Ultrasensitive Photodetector Based on a WSe ₂ /InSe Heterostructure by a Photogating Effect. ACS Applied Materials & Interfaces, 2021, 13, 50213-50219. | 4.0 | 26 |

| # | Article | IF | CITATIONS |
|----|--|------|-----------|
| 73 | Facile-synthesized carbonaceous photonic crystals/magnetic particle nanohybrids with heterostructure as an excellent microwave absorber. Journal of Alloys and Compounds, 2018, 741, 814-820. | 2.8 | 25 |
| 74 | Microwave absorbing properties of two dimensional materials GeP5 enhanced after annealing treatment. Applied Physics Letters, 2019, 114, . | 1.5 | 24 |
| 75 | Multistate Logic Inverter Based on Black Phosphorus/SnSeS Heterostructure. Advanced Electronic Materials, 2019, 5, 1800416. | 2.6 | 24 |
| 76 | Proximity Enhanced Hydrogen Evolution Reactivity of Substitutional Doped Monolayer WS ₂ . ACS Applied Materials & Interfaces, 2021, 13, 19406-19413. | 4.0 | 24 |
| 77 | Microwave absorption properties of heterostructure composites of two dimensional layered magnetic materials and graphene nanosheets. Applied Physics Letters, 2019, 115, . | 1.5 | 23 |
| 78 | Siliconâ€Phosphorusâ€Nanosheetsâ€Integrated 3Dâ€Printable Hydrogel as a Bioactive and Biodegradable Scaffold for Vascularized Bone Regeneration. Advanced Healthcare Materials, 2022, 11, e2101911. | 3.9 | 23 |
| 79 | Passively Q-switched ytterbium-doped ScBO ₃ laser with black phosphorus saturable absorber. Optical Engineering, 2016, 55, 081312. | 0.5 | 21 |
| 80 | Role of plastic deformation in tailoring ultrafine microstructure in nanotwinned diamond for enhanced hardness. Science China Materials, 2017, 60, 178-185. | 3.5 | 21 |
| 81 | Large topological Hall effect in nonchiral hexagonal MnNiGa films. Applied Physics Letters, 2017, 110, . | 1.5 | 21 |
| 82 | Photoluminescence and Raman Spectra Oscillations Induced by Laser Interference in Annealingâ€Created Monolayer WS ₂ Bubbles. Advanced Optical Materials, 2019, 7, 1801373. | 3.6 | 21 |
| 83 | Intensive suppression of thermal conductivity in Nd0.6Fe2Co2Sb12-xGex through spontaneous precipitates. Journal of Applied Physics, 2013, 114, 083715. | 1.1 | 20 |
| 84 | Novel three-dimensional boron nitride allotropes from compressed nanotube bundles. Journal of Materials Chemistry C, 2014, 2, 7022. | 2.7 | 20 |
| 85 | Carbonaceous photonic crystals as ultralong cycling anodes for lithium and sodium batteries. Journal of Materials Chemistry A, 2015, 3, 13786-13793. | 5.2 | 19 |
| 86 | Enhanced Stability of Black Phosphorus Fieldâ€Effect Transistors via Hydrogen Treatment. Advanced Electronic Materials, 2018, 4, 1700455. | 2.6 | 19 |
| 87 | Magnetic Anisotropy Control with Curie Temperature above 400 K in a van der Waals Ferromagnet for Spintronic Device. Advanced Materials, 2022, 34, e2201209. | 11.1 | 19 |
| 88 | Enhanced electromagnetic wave absorption properties of NiCo2 nanoparticles interspersed with carbon nanotubes. Journal of Magnetism and Magnetic Materials, 2019, 471, 185-191. | 1.0 | 18 |
| 89 | Synergistic Additiveâ€Assisted Growth of 2D Ternary In ₂ SnS ₄ with Giant Gateâ€Tunable Polarizationâ€&ensitive Photoresponse. Small, 2021, 17, e2008078. | 5.2 | 18 |
| 90 | Scalable Van der Waals Encapsulation by Inorganic Molecular Crystals. Advanced Materials, 2022, 34, e2106041. | 11.1 | 18 |

| # | Article | IF | CITATIONS |
|-----|---|-----|-----------|
| 91 | Formation, structure, and electric property of CaB4 single crystal synthesized under high pressure. Applied Physics Letters, 2010, 96, . | 1.5 | 17 |
| 92 | High pressure synthesis of Te-doped CoSb3 with enhanced thermoelectric performance. Journal of Materials Science: Materials in Electronics, 2015, 26, 385-391. | 1.1 | 17 |
| 93 | Strain Release Induced Novel Fluorescence Variation in CVD-Grown Monolayer WS ₂ Crystals. ACS Applied Materials & Interfaces, 2017, 9, 34071-34077. | 4.0 | 17 |
| 94 | Layered porous materials indium triphosphide InP3 for high-performance flexible all-solid-state supercapacitors. Journal of Power Sources, 2019, 438, 227010. | 4.0 | 17 |
| 95 | Highâ€Performance Broadband Photodetectors of Heterogeneous 2D Inorganic Molecular Sb ₂ O ₃ /Monolayer MoS ₂ Crystals Grown via Chemical Vapor Deposition. Advanced Optical Materials, 2020, 8, 2000168. | 3.6 | 17 |
| 96 | Coexistence of multiple metastable polytypes in rhombohedral bismuth. Scientific Reports, 2016, 6, 20337. | 1.6 | 16 |
| 97 | Si ₁₀ : A sp ³ Silicon Allotrope with Spirally Connected Si ₅ Tetrahedrons. Chemistry of Materials, 2016, 28, 6441-6445. | 3.2 | 16 |
| 98 | C ₆₀ on Nanostructured Nb-Doped SrTiO ₃ (001) Surfaces. Journal of Physical Chemistry C, 2010, 114, 3416-3421. | 1.5 | 15 |
| 99 | Low-Temperature Diffusion of Oxygen through Ordered Carbon Vacancies in Zr2Cx: The Formation of Ordered Zr2CxOy. Inorganic Chemistry, 2012, 51, 5164-5172. | 1.9 | 15 |
| 100 | {111}-specific twinning structures in nonstoichiometric ZrC _{0.6} with ordered carbon vacancies. Journal of Applied Crystallography, 2013, 46, 43-47. | 1.9 | 15 |
| 101 | Improved photoresponse and stable photoswitching of tungsten disulfide single-layer phototransistor decorated with black phosphorus nanosheets. Journal of Materials Science, 2017, 52, 11506-11512. | 1.7 | 15 |
| 102 | Facile Synthesis of Carbon-Encapsulated Ni Nanoparticles Embedded into Porous Graphite Sheets as High-Performance Microwave Absorber. ACS Sustainable Chemistry and Engineering, 2018, 6, 16179-16185. | 3.2 | 15 |
| 103 | Mechanical Robustness Two-Dimensional Silicon Phosphide Flake Anodes for Lithium Ion Batteries. ACS Sustainable Chemistry and Engineering, 2020, 8, 17597-17605. | 3.2 | 15 |
| 104 | Annealing-Induced {011}-Specific Cyclic Twins in Tetragonal Zirconia Nanoparticles. Journal of Physical Chemistry C, 2012, 116, 21052-21058. | 1.5 | 14 |
| 105 | Interlayer exchange coupling and magnetic reversal in Co/Pt multilayers. Journal of Magnetism and Magnetic Materials, 2013, 325, 117-121. | 1.0 | 14 |
| 106 | Grain wall boundaries in centimeter-scale continuous monolayer WS ₂ film grown by chemical vapor deposition. Nanotechnology, 2018, 29, 255705. | 1.3 | 14 |
| 107 | New hexagonal boron nitride polytypes with triple-layer periodicity. Journal of Applied Physics, 2017, 121, . | 1.1 | 13 |
| 108 | Simple preparation and excellent microwave attenuation property of Fe3O4- and FeS2- decorated graphene nanosheets by liquid-phase exfoliation. Journal of Alloys and Compounds, 2019, 810, 151881. | 2.8 | 13 |

| # | Article | IF | CITATIONS |
|-----|--|------|-----------|
| 109 | One-step growth of wafer-scale monolayer tungsten disulfide via hydrogen sulfide assisted chemical vapor deposition. Applied Physics Letters, 2019, 115, . | 1.5 | 13 |
| 110 | Photodetection application of one-step synthesized wafer-scale monolayer MoS2 by chemical vapor deposition. 2D Materials, 2020, 7, 025020. | 2.0 | 13 |
| 111 | High-sensitivity and versatile plasmonic biosensor based on grain boundaries in polycrystalline 1L WS2 films. Biosensors and Bioelectronics, 2021, 194, 113596. | 5.3 | 13 |
| 112 | Synthesis of B–C–N nanocrystalline particle by mechanical alloying and spark plasma sintering. Journal of Materials Science, 2006, 41, 8352-8355. | 1.7 | 12 |
| 113 | Deep melting reveals liquid structural memory and anomalous ferromagnetism in bismuth. Proceedings of the National Academy of Sciences of the United States of America, 2017, 114, 3375-3380. | 3.3 | 12 |
| 114 | One-Step Growth of Spatially Graded Mo _{1–<i>x</i>} W _{<i>x</i>} S ₂ Monolayers with a Wide Span in Composition (from <i>x</i> = 0 to 1) at a Large Scale. ACS Applied Materials & Interfaces, 2019, 11, 20979-20986. | 4.0 | 12 |
| 115 | First-Principles Investigation of Dense B ₄ C ₃ . Journal of Physical Chemistry C, 2007, 111, 13679-13683. | 1.5 | 11 |
| 116 | Metastable adaptive orthorhombic martensite in zirconia nanoparticles. Journal of Applied Crystallography, 2014, 47, 684-691. | 1.9 | 11 |
| 117 | Pressure Effect on Order–Disorder Ferroelectric Transition in a Hydrogen-Bonded Metal–Organic Framework. Journal of Physical Chemistry Letters, 2020, 11, 9566-9571. | 2.1 | 11 |
| 118 | The rise of plastic deformation in boron nitride ceramics. Science China Materials, 2021, 64, 46-51. | 3.5 | 11 |
| 119 | In Situ Grown Ultrafine RuO ₂ Nanoparticles on GeP ₅ Nanosheets as the Electrode Material for Flexible Planar Micro-Supercapacitors with High Specific Capacitance and Cyclability. ACS Applied Materials & Interfaces, 2021, 13, 47560-47571. | 4.0 | 11 |
| 120 | Distinct C60 growth modes on anthracene carboxylic acid templates. Applied Physics Letters, 2010, 96, 143115. | 1.5 | 10 |
| 121 | Tian et al. reply. Nature, 2013, 502, E2-E3. | 13.7 | 10 |
| 122 | Multifunctional Photodetectors Based on Nanolayered Black Phosphorus/SnS _{0.5} Se _{1.5} Heterostructures. ACS Applied Nano Materials, 2019, 2, 3548-3555. | 2.4 | 10 |
| 123 | High-performance flexible all-solid-state micro-supercapacitors based on two-dimensional InSe nanosheets. Journal of Power Sources, 2021, 482, 228987. | 4.0 | 10 |
| 124 | Extreme mechanical anisotropy in diamond with preferentially oriented nanotwin bundles. Proceedings of the National Academy of Sciences of the United States of America, 2021, 118, . | 3.3 | 10 |
| 125 | Magnetoresistance and Anomalous Hall Effect with Pt Spacer Thickness in the Spin-Valve Co/Pt/[Co/Pt]2 Multilayers. Journal of Superconductivity and Novel Magnetism, 2017, 30, 533-538. | 0.8 | 9 |
| 126 | Accelerated Degradation of CrCl ₃ Nanoflakes Induced by Metal Electrodes: Implications for Remediation in Nanodevice Fabrication. ACS Applied Nano Materials, 2019, 2, 1597-1603. | 2.4 | 9 |

| # | Article | IF | CITATIONS |
|-----|--|------------------|---------------|
| 127 | Prediction of a conducting hard ductile cubic IrC. Physica Status Solidi - Rapid Research Letters, 2010, 4, 230-232. | 1.2 | 8 |
| 128 | Strengthening in high-pressure quenched Zr. High Pressure Research, 2017, 37, 278-286. | 0.4 | 8 |
| 129 | Two-dimensional layered materials InSe nanoflakes/carbon nanotubes composite for flexible all-solid-state supercapacitors. Journal of Materials Science, 2020, 55, 2947-2957. | 1.7 | 7 |
| 130 | Influence of van der Waals epitaxy on phase transformation behaviors in 2D heterostructure. Applied Physics Letters, 2020, 116, . | 1.5 | 7 |
| 131 | Carbonaceous photonic crystals prepared by high-temperature/hydrothermal carbonization as high-performance microwave absorbers. Journal of Materials Science, 2019, 54, 14343-14353. | 1.7 | 6 |
| 132 | Recent advances in exchange bias of layered magnetic FM/AFM systems. Science China: Physics, Mechanics and Astronomy, 2013, 56, 61-69. | 2.0 | 5 |
| 133 | Weak antilocalization effect in exfoliated black phosphorus revealed by temperature- and angle-dependent magnetoconductivity. Journal of Physics Condensed Matter, 2018, 30, 085703. | 0.7 | 5 |
| 134 | Hydrogen Bond Tuning of Magnetoelectric Coupling in Metal–Organic Frameworks. Journal of Physical Chemistry C, 2020, 124, 16111-16115. | 1.5 | 5 |
| 135 | Broadband light absorption and photoresponse enhancement in monolayer WSe2 crystal coupled to Sb2O3 microresonators. Nano Research, 2022, 15, 4653-4660. | 5.8 | 5 |
| 136 | Ferroelectrics: Nonvolatile Ferroelectric Memory Effect in Ultrathin αâ€In 2 Se 3 (Adv. Funct. Mater.) Tj ETQq0 0 | 0 rgBT /O 7.8 | verlock 10 Tf |
| 137 | Direct one-step synthesis of CoFex@Co@C hybrids derived from a metal organic framework for a lightweight and high-performance microwave absorber. Nanotechnology, 2020, 31, 095703. | 1.3 | 4 |
| 138 | Peculiar spectra and photocurrent oscillation caused by laser interference in WX2 (X = S, Se) bubbles. Journal of Materials Science, 2020, 55, 15857-15866. | 1.7 | 4 |
| 139 | Nonlinear optical response of a monolayer WS ₂ and the application of a hundred-MHz nanosecond laser. Optics Express, 2021, 29, 36634. | 1.7 | 4 |
| 140 | Pressure Control of the Structure and Multiferroicity in a Hydrogen-Bonded Metal–Organic Framework. Inorganic Chemistry, 0, , . | 1.9 | 4 |
| 141 | Pressure effect on spin-driven multiferroicity in a Y-type hexaferrite. Journal of Materials Chemistry C, 2019, 7, 4173-4177. | 2.7 | 3 |
| 142 | Magnetism and microwave absorption properties of two-dimensional layered ferromagnetic metal Fe3GeTe2. Journal of Materials Science, 2021, 56, 16524-16532. | 1.7 | 3 |
| 143 | Current-induced torques in black phosphorus/permalloy bilayers due to crystal symmetry. Applied Physics Letters, 2020, 117, 062403. | 1.5 | 2 |
| 144 | Controllable growth of multilayered XSe ₂ (X = W and Mo) for nonlinear optical and optoelectronic applications. 2D Materials, 2022, 9, 015012. | 2.0 | 2 |

| # | Article | IF | CITATIONS |
|-----|---|------|-----------|
| 145 | Heat Treatment Effect on the Magnetic Properties of Cu-Nb Micro-Composites. IEEE Transactions on Applied Superconductivity, 2012, 22, 6002004-6002004. | 1.1 | 1 |
| 146 | Carbon Vacancy Ordered Non-Stoichiometric ZrC0.6. , 2013, , 478-508. | | 1 |
| 147 | Chemical synthesis and characterization of MnO ₂ -coated Co nanoparticles. Journal of Materials Research, 2010, 25, 1748-1754. | 1.2 | Ο |
| 148 | Chemical synthesis and characterization of manganese oxide coated Ni particles. Science China: Physics, Mechanics and Astronomy, 2013, 56, 1508-1513. | 2.0 | 0 |
| 149 | n -Dependent variations of coercivity with temperature in [Co/Pt] n multilayers. Applied Surface Science, 2015, 345, 182-186. | 3.1 | Ο |
| 150 | Photoemission oscillation in epitaxially grown van der Waals β-In ₂ Se ₃ WS ₂ heterobilayer bubbles*. Chinese Physics B, 2021, 30, 117901. | 0.7 | 0 |
| 151 | Carbon Vacancy Ordered Non-Stoichiometric ZrC0.6. , 0, , 667-689. | | 0 |
| 152 | Scalable Van der Waals Encapsulation by Inorganic Molecular Crystals (Adv. Mater. 7/2022). Advanced Materials, 2022, 34, . | 11.1 | 0 |